Towards Mimetic Membrane Systems in Molecular Dynamics: Characteristics of *E. coli* Membrane System

Mateusz Rzycki[1,2] [0000-0003-3655-3048] , Sebastian Kraszewski[2] [0000-0003-3244-7694] , Dominik Drabik[2,3] [0000-0003-4568-4066]

[1] Wroclaw University of Science and Technology, Faculty of Fundamental Technical Problems, Department of Experimental Physics, Wroclaw, Poland
[2] Wroclaw University of Science and Technology, Faculty of Fundamental Technical Problems, Department of Biomedical Engineering, Wroclaw, Poland
[3] Laboratory of Cytobiochemistry, Faculty of Biotechnology, University of Wroclaw, Wroclaw, Poland
mateusz.rzycki@pwr.edu.pl

Abstract. Plenty of research is focused on the analysis of the interactions between bacteria membrane and antimicrobial compounds or proteins. The hypothesis of the research is formed according to the results from the numerical models such as molecular docking or molecular dynamics. However, simulated membrane models often vary significantly from the real ones. This may lead to inaccurate conclusions. In this paper, we employed molecular dynamic simulations to create a mimetic *Escherichia coli* full membrane model and to evaluate how the membrane complexity may influence the structural, mechanical and dynamical mainstream parameters. The impact of the O-antigen region presence in the outer membrane was also assessed. In the analysis, we calculated membrane thickness, area per lipid, order parameter, lateral diffusion coefficient, interdigitation of acyl chains, mechanical parameters such as bending rigidity and area compressibility, and also lateral pressure profiles. We demonstrated that outer membrane characteristics strongly depend on the structure of lipopolysaccharides, changing their properties dramatically in each of the investigated parameters. Furthermore, we showed that the presence of the inner membrane during simulations, as it exists in a full shell of *E. coli*, significantly changed the measured properties of the outer membrane.

Keywords: Molecular dynamics, mimetic systems, lipid membrane model

1 Introduction

Escherichia coli is one of the most frequently investigated bacteria being responsible for common infections among humans and animals [1, 2]. This strain is widely used for antimicrobial studies [3–5]. It belongs to the Gram-negative ones which membranes consist of the outer (OM) and the inner membrane (IM) separated by the periplasm. OM is an asymmetric bilayer primarily composed of lipopolysaccharides (LPS) in the top leaflet and phospholipids (PL) in the bottom one [6]. It serves as a protective shield

ICCS Camera Ready Version 2021
To cite this paper please use the final published version:
DOI: 10.1007/978-3-030-77964-1_42

preventing the entry of toxic compounds e.g. antibiotics [7, 8]. The LPS is composed of three segments: lipidA-the hydrophobic fatty surface forming the base of the top OM leaflet, a phosphorylated, highly anionic core and an O-antigen unit composed of sugar chains performing a hydrophilic surface [7, 9]. IM has a dynamic structure mostly formed by phosphatidylethanolamine (PE), phosphatidylglycerol (PG) and cardiolipin (CL) [10, 11].

In computational studies on bacteria membranes, methods such as molecular dynamics are often employed [12]. This allows observation of the behavior of studied molecules up to the atomic level. However, many modelled systems are simplified and limited to one particular membrane even for Gram-negative bacteria [13–16]. Piggot *et al.* performed the analysis on the base model of OM *E. coli* with embedded FecA protein, presenting the LPS structure on the upper leaflet, while the lower one was composed of PE and PG [15]. A similar model was proposed by Wu *et al.* a few years earlier where a couple of LPS structures were studied [13]. One of the most comprehensive approaches was delivered by Hwang *et al.* where the two – inner and outer membranes were separately modelled and analyzed [14]. While those models are quite close to reality, they may significantly differ from the real OM/IM bacterial membrane or even experimental models. This may result in influencing the outcome results.

In this work, we investigate the changes in membrane properties with the increasing complexity of the systems to better reflect bacterial membrane and to draw attention that both OM and IM should not be studied separately for better biological context. For this purpose, we created five bacterial membrane models based on the composition of *E. coli*. We started from simple pure IM and pure OM (with and without O-antigen units used). To better reflect the natural conditions we created whole OM/IM bacteria membrane system (first without O-antigen units and latter with O-antigen units). Each of the systems was analyzed in detail to characterize the topological and mechanical properties of the membranes in investigated systems and to present the influence on how structural complexity can affect membrane behavior.

2 Methods

The all-atom models of the membranes were generated using CHARMM-GUI membrane builder [17]. The IM model consisted of 80% PYPE, 15% PYPG, 5% PVCL2 [10, 11, 18]. The lipid bilayer was solvated with TIP3P water molecules (100 water molecules per lipid) and 240 mM NaCl were added based on literature data [19]. Final IM configuration included: 256 PYPE, 48 PYPG, 16 PVCL2, 276 Na^+, 196 Cl^- and 32000 TIP3P molecules.

The OM models were composed of 75% PYPE and 25% PYPG in the upper leaflet and 100% LPS in the lower one [13, 20]. The type1 of lipidA, R1 core and repeating units of O6-antigen were included in the LPS sequence. The length of the O6-antigens was adapted based on results published by Wu *et al.* [13, 21]. The number of LPS molecules and phospholipids was equally adjusted to the total lipid area occupied on each leaflet. The same procedure of solvation and ion addition was employed as before, except for Ca^{2+} ions, which were automatically added based on LPS length to neutralize

ICCS Camera Ready Version 2021
To cite this paper please use the final published version:
DOI: 10.1007/978-3-030-77964-1_42

the system. Afterward, molecular dynamics (MD) simulations of two asymmetric LPS based bilayers were performed. The upper leaflet contained: lipidA, R1 core and 2 repeating units of O6-antigen (OMA) and lipidA, R1 core (OM0). Final OMA and OM configuration included: 52 LPS, 120 PYPE, 40 PYPG, 260 Ca^{2+}, 232 Na^{+}, 112 Cl^{-}, 28964 TIP3, and 60 LPS, 144 PYPE, 48 PYPG, 300 Ca^{2+}, 168 Na^{+}, 120 Cl^{-} and 27856 TIP3P molecules respectively. Three-dimensional periodic boundary conditions were applied to deal with potential energy disruption due to the origin of cell discontinuity.

MD simulations of pure membranes were performed using the GROMACS (version 2020.4) package with the CHARMM36 force field [22, 23]. Each system was first minimized using the steepest descent algorithm for energy minimization. Calculations were carried out in the NPT ensemble (constant Number of particles, Pressure and Temperature) using a Nose-Hoover thermostat at T=303.15 K and semi-isotropic coupling with Parrinello-Rahman barostat at p =1bar. The long-run production was conducted for at least 300 ns using the leap-frog integrator. Chemical bonds between hydrogen and heavy atoms were constrained to their equilibrium values by the LINCS algorithm, while long-range electrostatic forces were evaluated using the particle mesh Ewald (PME) method, which allowed us to employ the integration timestep of 2 fs.

The complete bacterial membrane models: LIPA (IM+OMA) and LIP0 (IM+OM0) have been constructed by assembling IM and OM separated by a small water slab (2.4 nm, 4140 water molecules) imitating the periplasm. The minimization procedure and NPT ensemble were carried out according to the same protocol as described above. We analyzed the last 10ns of all simulations using a combination of GROMACS tools, self-made MATLAB (The MathWorks, Natick, MA) scripts, VMD and VMD's dedicated plugins such as MEMBPLUGIN 1.1 [24] for interdigitation calculation.

The order parameter of the acyl chains was obtained using:

$$S_{CH} = \frac{3}{2}\langle cos^2\,\theta\rangle - \frac{1}{2} \tag{1}$$

where θ for a particular carbon atom is the angle between the bilayer normal and carbon-hydrogen bond.

The diffusion was calculated in the Diffusion Coefficient Tool [25] from the slope of the mean-squared displacement (MSD) curve through Einstein's relation. For the computation accuracy, only phosphorous atoms of all lipids were taken into account.

$$D(\tau) = \frac{M(\tau)}{2E\tau} \tag{2}$$

where $M(\tau)$ – is the MSD at a range of lag time τ and E represents the dimensionality (two in our case - XY).

Lateral Pressure profiles (LPPs) were computed using a custom version of GROMACS-LS [26]. The obtained beforehand trajectories were adapted to comply with the software requirements, thus the calculations of the PME electrostatic forces were settled to cutoff. We also adjusted the cutoff to 2.2nm according to Vanegas *et al.* [26, 27]. The lateral component of pressure tensor ($P_L(z) = 0.5 \times (P_{xx}(z) + P_{yy}(z))$) and

ICCS Camera Ready Version 2021
To cite this paper please use the final published version:
DOI: 10.1007/978-3-030-77964-1_42

the normal component ($P_N = P_{zz}$) are computed from the GROMACS-LS output. Finally, LPPs $\pi(z)$ was determined from:

$$\pi(z) = P_L(z) - P_N. \quad (3)$$

Bending rigidity was determined using the real space fluctuation method [28]. Briefly, a probability distribution for both tilt and splay is determined for all lipids over the last 10ns of simulation. Tilt is defined as an angle between the lipid director (vector between lipid head – the midpoint between C2 and P atoms – and lipid tail – the midpoint between last carbon atoms) and bilayer normal. Lipid splay is defined as divergence of an angle formed by the directors of neighboring lipids providing that they are weakly correlated. Area compressibility was determined using a method developed by Doktorova *et al.* [29]. Briefly, a real-space analysis of local thickness fluctuations is sampled from the simulations.

Determined parameters' statistical significance was performed using one-way ANOVA significance test with Tukey post hoc test in Origin 2018 (OriginLabs) software.

3 Results

Each of the investigated systems was characterized thoroughly. In the Fig. 1 and Fig. 2 we present LIPA and LIP0 systems in detail, including their density profiles and graphical representation. Structural, stress and mechanical parameters of lipid membranes were determined. We studied whether simplification of biological membranes, which is common for numerical simulations, is feasible. We assume that significant differences between the systems may result in the different occurrence of biological phenomena.

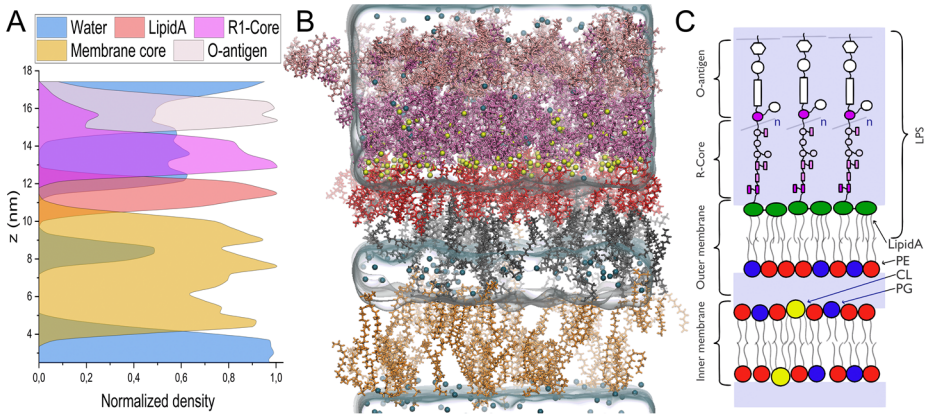

Fig. 1 A) Density profile of LIPA regions. B) LIPA system visualization (several lipids are hidden for clarity). The Inner membrane, outer membrane, lipidA, R-Core, O-antigen region, water, calcium ions, sodium together with chlorine ions have been colored orange, gray, red, magenta, pink, azure, yellow and dark blue, respectively. C) Graphical representation of created LIPA system.

ICCS Camera Ready Version 2021
To cite this paper please use the final published version:
DOI: 10.1007/978-3-030-77964-1_42

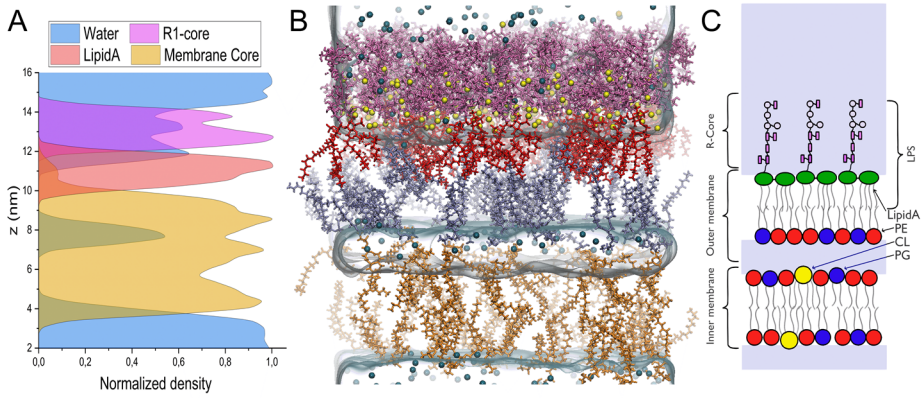

Fig. 2 A) Density profile of LIP0 regions. B) LIP0 system visualization (several lipids are hidden for clarity). The inner membrane, outer membrane, lipidA, R-Core, water, calcium ions, sodium together with chlorine ions have been colored in orange, ice blue, red, magenta, azure, yellow and dark blue, respectively. C) Graphical representation of created LIP0 system.

For the structural aspect of the membrane, we decided to perform a standard analysis with a couple more comprehensive parameters afterward. To understand and characterize the molecular effect of LPS on the membrane and/or additional membrane in complex systems, we determined different bilayer properties such as membrane thickness (MT), area per lipid (APL), order parameter, interdigitation and lateral diffusion. Membrane thickness was determined between phosphorus atoms, while the area per lipid was determined using Voronoi tessellation. The results of structural characteristics are presented in Table 1. All of the parameters were statistically distinct.

Further structural characterization was enhanced with a description of lipid behavior in the systems. For this purpose, lateral mobility, which is usually described by the lateral diffusion coefficient, was investigated. The diffusion coefficient from the 2D mean square displacement equation was calculated. Obtained values were statistically significantly different between the investigated systems. Finally, the determination of acyl chain interdigitation to assess interactions between the leaflets itself was performed. The parameter allows estimating whether O-antigens presence may influence the interactions between the leaflets. As before the differences in values of interdigitation were statistically significant between the investigated systems.

Additionally, to provide a wider insight into the flexibility of the acyl chains, the order parameter was calculated. Presented values were averaged over the whole trajectories for clarity and collected in Table 2. We report values for the sn-2 unsaturated chain in the following manner: initial atoms in the acyl chain (Start), atoms before double bond (Midpoint), and the final (End). Standard deviations are not included, since in all cases are below 0.02.

ICCS Camera Ready Version 2021
To cite this paper please use the final published version:
DOI: 10.1007/978-3-030-77964-1_42

Table 1 Comparison of structural and dynamic parameters between pure and complex membranes [a].

Membrane	Lipid type	MT_{P-P}	APL_1	APL_2	Interdigitation	Diffusion
		Å	Å^2	Å^2	Å	µm/s
IM	Total	39.9±0.4	56.6±1.8	58±2	4.9±0.4	-
	PYPE		58±1	59.1±0.6		12.0±0.1
	PYPG		63±2	61.7±2.3		15.8±0.1
	PVCL2		88±4	78±4		12.8±0.1
OMA	Total	35.5±0.2	194.2±3.3	60.3±1.9	5.0±0.3	-
	PYPE		-	60.8±0.7		6.4±0.1
	PYPG		-	66.5±2.0		6.1±0.1
	LipidA		194.2±3.3	-		0.6±0.1
OM0	Total	37.2±0.2	183±2	55.6±1.5	4.3±0.2	-
	PYPE		-	56.4±0.4		10.0±0.1
	PYPG		-	59.7±1.3		7.7±0.2
	LipidA		183±2	-		0.9±0.1
LIPA	Outer	33.3±0.6	183±3	59±1	4.9±0.4	-
	PYPE		-	64.7±0.6		2.8±0.0
	PYPG		-	66.5±1.1		3.2±0.2
	LipidA		183±3	-		0.3±0.1
	Inner	35.0±0.7	55±2	62.8±2.4	5.0±0.3	-
	PYPE		59±1	61±1		8.4±0.1
	PYPG		63±3	65±2		11.3±0.2
	PVCL2		65±2	75±3		10.2±0.3
LIP0	Outer	35.3±0.4	182.7±4.4	59.6±1.1	7.1±0.5	-
	PYPE		-	63.9±0.5		3.4±0.1
	PYPG		-	67±1		4.2±0.1
	LipidA		182.7±4.4	-		0.2±0.1
	Inner	38.8±0.4	61.3±2.2	65±2	5.9±0.2	-
	PYPE		62.4±0.6	63.3±0.7		7.0±0.1
	PYPG		60.1±1.5	70±2		9.0±0.1
	PVCL2		75±3	82±3		12.7±0.1

[a] MT_{P-P} - membrane thickness measure between phosphorous atoms from opposite leaflets; APL1, APL2 - the area per lipid on the upper and lower leaflet, respectively; IM – inner membrane; OM0 – outer membrane without antigens; OMA – outer membrane with antigens; LIP0 – mimetic *E. coli* system without antigens; LIPA – mimetic *E. coli* system with O-antigens.

ICCS Camera Ready Version 2021
To cite this paper please use the final published version:
DOI: 10.1007/978-3-030-77964-1_42

Table 2 Acyl chain order parameter from pure and complex systems.

Membrane	Lipid type	Order parameter		
		Start	Midpoint	End
IM	PYPE	0.24	0.13	0.12
	PYPG	0.23	0.13	0.12
	PVCL	0.20	0.11	0.09
OM0	PYPE	0.24	0.13	0.12
	PYPG	0.25	0.13	0.12
	LipidA	0.20	0.15	0.10
OMA	PYPE	0.20	0.10	0.08
	PYPG	0.21	0.10	0.10
	LipidA	0.17	0.14	0.07
LIP0	PYPE	0.20	0.09	0.08
	PYPG	0.19	0.11	0.09
	PVCL	0.22	0.09	0.07
	PYPE	0.20	0.09	0.08
	PYPG	0.19	0.11	0.09
	LipidA	0.20	0.23	0.13
LIPA	PYPE	0.22	0.12	0.10
	PYPG	0.21	0.11	0.09
	PVCL	0.23	0.09	0.08
	PYPE	0.22	0.12	0.10
	PYPG	0.22	0.11	0.09
	LipidA	0.18	0.17	0.08

Stress characterization was done by evaluation of the stress profile along bilayer normal and determination of the lateral pressure profile (LPP) $\pi(z)$. As a reference, we present Fig. 3 where the lateral pressure profile of OM's and LIPA combined with pure IM and OMA was calculated. For other systems, we collected the peak values (see Table 3).

The introduced LPPs indicate a similar tendency between basic and complex membrane. Starting from the bulk solvent, the first minor positive peak may be distinguished as a water-headgroup interface (I), indicating the repulsive forces from lipids. Further, the negative peak (II) is visible presenting glycerol region, including attractive hydrophobic forces [30], while subsequent major peak denotes the acyl chain region (III) and finish at the bilayer center nearby 6 nm (IV).

ICCS Camera Ready Version 2021
To cite this paper please use the final published version:
DOI: 10.1007/978-3-030-77964-1_42

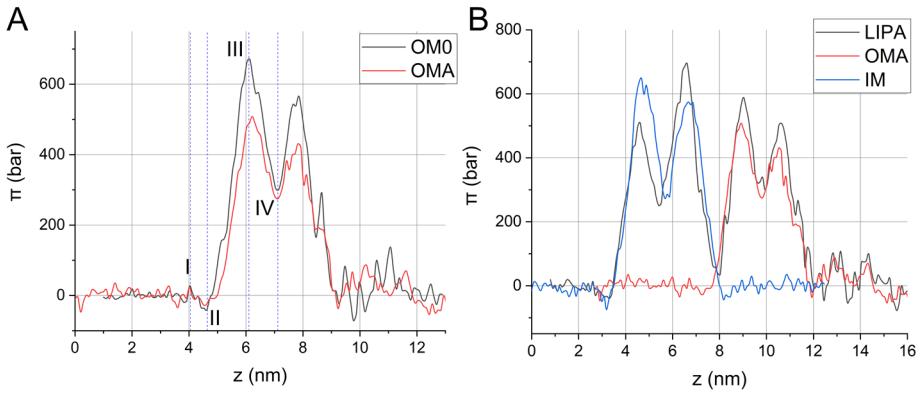

Fig. 3 Lateral pressure profile of A) OM0 and OMA, B) LIPA system with corresponding pure bilayer components OMA and IM.

Finally, mechanical characterization of membranes is performed. Such characterization allows assessing very subtle changes induced by sugar-coating of LPS or additional membrane complexity. Both area compressibility (K_A) and bending rigidity (κ) are determined (see Table 3). All reported values are statistically significantly different.

Table 3 Mechanical and pressure properties of pure and complex systems [b].

Membrane	κ	κ_{tilt}	K_{A1}	K_{A2}	K_A	Lateral pressure
	kbT	kbT	mN/m	mN/m	mN/m	bar
IM	22.1±0.6	10.6±0.3	133±20	133±17	133±15	647±21
OMA	22.7±0.4	13.3±0.4	18±12	84±27	29±10	508±11
OM0	29.2±0.4	17.1±0.2	57±6	141±34	81±18	670±30
LIPA						
outer	25.0±0.5	15.8±0.6	41.7± 5.3	126.3±5.4	62.7±5.2	588±16
inner	16±1	4.8±0.3	165±24	31±23	51±20	695±14
LIP0						
outer	26.4±0.9	15.0±0.7	58.8±4.6	86.2±7.1	70.0±5.4	690±26
inner	16.8±0.4	7.3±0.8	34±9	42±27	37±17	533±21

[b] κ – bending rigidity; κ_{tilt} – tilt; K_{A1}, K_{A2}, K_A - compressibility of the upper leaflet, lower leaflet, and total membrane, respectively; IM – inner membrane; OM0 – outer membrane without antigens; OMA – outer membrane with antigens; LIP0 – mimetic *E. coli* system without antigens; LIPA – mimetic *E. coli* system with antigens.

ICCS Camera Ready Version 2021
To cite this paper please use the final published version:
DOI: 10.1007/978-3-030-77964-1_42

4 Discussion

For a comprehensive analysis, we decided to divide the discussion section into two subsections. First, we focus on the impact of the O-antigen segment on the asymmetric outer membrane. Next, we draw attention to the discrepancies in the complete bacterial membrane systems compared to single membrane model systems.

4.1 The effect of the O-antigen region presence on the outer membrane parameters

In the outer membrane systems, we observe significant differences between OM0 and OMA, as the latter one is equipped with an extra O-antigen region. The presence of that structure induces membrane thickness reduction and APL extension in the upper leaflet (see Table 1). Interestingly, this directly influences the lower leaflet, where the total APL is lower than in the corresponding leaflet in OM0 system. The change of membrane thickness is proportional to the interdigitation of the acyl chains in the outer bilayer. We may conclude that the reduction in bilayer thickness is accompanied by the growth of the interdigitation [31]. The presence of O-antigens increases the interdigitation between the lipidA and PE:PG leaflets, which is followed by thickness reduction. However, analysis of the interdigitation in asymmetric membranes with the LPS layer is not straightforward. Shearer *et al.* suggested that the properties of OM systems are much more dependent on the dynamics and structure of the LPS segment [32].

The diffusion coefficient analysis showed a significant difference between OMA and OM0 systems as well. The occurrence of additional sugar coating substantially limits the mobility of the whole membrane. It remains consistent with the previous works [33–35]. The O-antigen essentially impacts the lower leaflet of the outer membrane, since PE and PG fluidity is restricted by 36% and 21%, respectively.

The calculated order parameter indicated that in both cases ordering trend is decreasing toward the bilayer center (see Table 2), our results are consistent with the ones presented by Wu *et al.* [13]. Interestingly the presence of the O-antigen segment affects membranes as values on both leaflets are lower.

Both OMA and OM0 exhibit a similar pressure trend along the bilayer normal (see Fig. 3). Noteworthy, much higher lateral stress was denoted at the lower leaflet at the OM0 system, reaching the top value of 670±30 bar, while on OMA only 508±11 bar was observed. Since the presented membranes are not symmetric, the lateral pressure on the upper and lower leaflets varies, however, both in a similar manner. A slightly noticeable shift at the bilayer center represents the interdigitation parameter of both membranes and remains consistent with values in Table 1. Since the interdigitation in OMA acyl chains is more intense, the plot downhill is deeper. Since the presence of the antigens in the membrane decreases the lateral pressure and lateral diffusion, this change could have a significant influence on the behavior of the system. Changes in both parameters could influence for instance membrane transport [36].

The presence of antigens in the LPS leaflet induced significant mechanical changes (see Table 3). All of the parameters - bending rigidity, tilt, and compressibility - were

ICCS Camera Ready Version 2021
To cite this paper please use the final published version:
DOI: 10.1007/978-3-030-77964-1_42

lower when O-antigens were present compared to the membrane without antigens. Such a difference is not surprising, as additional O-antigens are in the water part of the system, hence exposing the leaflet to additional repulsive forces, making the structure less resistant and exhibiting more fluctuations. Since lateral diffusion and lateral pressure are lower when antigens are present it can be concluded that membrane is, at least in the interphase region, more ordered. Such a conclusion cannot be made for the acyl chain region, as interdigitation increases when O-antigens are present.

4.2 The comparison of *E. coli* membrane models

The models presented in this study require a detailed analysis of their topological and mechanical characteristics. To this end, we decided to compare those properties for both inner and outer membranes from the *E. coli* models to pure ones. Taking into account the entire set of membranes, LIPA and LIP0 exhibit reduced bilayer thickness in both inner and outer membrane cases. Major differences we observe between pure IM and LIPA where the thickness reduction was supported with cardiolipin (CL) APL decrement of 12.3% (4.9Å) and 26.1% (23Å^2), respectively (see Table 1). In LIP0 structure modifications occurred in the inner membrane and the lower leaflet of the outer one when comparing APL and thickness parameters. Interestingly, significant reduction may be observed in the upper leaflet of the LIPA outer membrane, since lipidA reduced APL by 10 Å^2. Analysis of the interdigitation parameter between acyl chains from opposite leaflets seems to be slightly different than before. Obtained values from the LIPA system did not vary enough and were not significant compared to IM and OMA models with extra O-antigens. Thus, this parameter is not sensitive to the complexity of the membranes. However, the opposite pathway has been presented in LIP0 system. The interdigitation pitched up by 20.4% (to 5.9±0.2Å) on IM and by 65.1% (to 7.1±0.5Å) on OM, respectively. Similarly, as before this phenomenon is inversely correlated to the bilayer thickness, where the decrease is accompanied by the interdigitation increase. We confirmed that the presence of O-antigens escalates the interdigitation between acyl chains from the opposite leaflet, followed by thickness reduction.

Furthermore, investigation of the diffusion coefficient revealed that in comprehensive models LIPA and LIP0 the mobility of the lipid particles is substantially limited. In LIP0, PE and lipidA fluidity was almost three and four times reduced, compared to OM0. A similar situation appears when analyzing LIPA and OMA, PE and lipidA mobility is limited more than twice in both cases. In pure OMA long sugar chains O-antigen reduce the fluidity of the whole membrane, which is accompanied by a corresponding interdigitation parameter. Further, the difference in fluidity of OMA and OM0 outer membranes was reduced in the whole bacteria systems.

Noteworthy the ordering of acyl chains is not as clear as, on pure outer membranes, observed fluctuations in several cases are not statistically significant (see Table 2). However, we indicate that the sn-2 ordering in the inner membrane of both LIPA and LIP0 compared to pure IM significantly decreased.

Afterward, we compared the LPPs of the LIPA and LIP0 to indicate the stress tensor contrasts resulted from O-antigen presence (see Fig 3). Pure IM exhibits higher lateral stress at the lower leaflet since extreme values are reached compared to the LIPA

ICCS Camera Ready Version 2021
To cite this paper please use the final published version:
DOI: 10.1007/978-3-030-77964-1_42

membrane. Marginal shifts at the bilayer center represent the interdigitation of both membranes and remain consistent with values in Table 1. Finally, LIPA reaches the top stress value of 695±14 bar at the upper leaflet of the inner membrane. Pressure on the outer membrane was lower than in the case of the inner. In LIPA the total lateral pressure in the inner and outer membrane is higher compared to pure ones (IM and OMA) and it was interestingly distributed mostly on adjacent leaflets. In our opinion growth of pressure on the upper leaflet from the inner membrane and the lower leaflet from the outer membrane supports the complex system formation, while the highest lateral stress occurs there.

Moving forward to the mechanical characterization the differences in mechanical properties are also statistically significant when the additional membrane is present in the system (see Table 3). Obtained $\boldsymbol{\kappa}$ values from pure systems are consistent with those delivered by Hsu *et al.* [33]. In the case of IM bending rigidity was lower in IM of both LIPA and LIP0 when compared to the model IM system. The opposite tendency was observed in the case of area compressibility where IM of LIPA and LIP0 had, in general, lower values than in the model system. Similar to Jefferies *et al.* we notice that various LPS composition differ in the matter of mechanical strength or mobility [37]. Differences can be observed in the case of OM, however, due to the presence of antigens, the tendency is less straightforward. Bending rigidity values of OM in LIPA and LIP0 systems are in between the values of the model OM system with and without O-antigens. This suggests that additional bilayer in the system stabilizes the system with antigens but also increases the whole dynamics of the membrane without antigens. This is also valid for the area compressibility parameter of whole membranes, however, became more complicated to evaluate when individual leaflet compressibilities were taken into account. Nevertheless, it should be noted that the presence of the second membrane in the simulated system strongly affected the mechanical behavior of both membranes when compared to single membrane model systems, and should be considered in numerical studies for better biological context.

5 Conclusions

In this paper, we performed a detailed study of structural, mechanical and stress parameters of lipid membranes mimicking the *E. coli* dual membrane system. We showed the changes of numerically determined parameters with progressive complexity of the membrane systems. We presented that LPS-rich outer membrane properties strongly depend on the structure of LPS itself, changing dramatically each of the investigated parameters. Furthermore, we showed that the presence of the second (inner) membrane, mimicking the OM/IM relation in *E. coli*, significantly influenced primary membrane properties as well. Such changes may be crucial for interaction origins between particles and the membrane. As a result, common biological phenomena could not be observed numerically - or will behave differently from reality - if the simplified membrane model is used in the simulation. In future perspectives, the interactions of membrane-active particles and membranes in various membrane mimetic systems should be investigated.

ICCS Camera Ready Version 2021
To cite this paper please use the final published version:
DOI: 10.1007/978-3-030-77964-1_42

ACKNOWLEDGEMENTS

M.R and S.K. acknowledge support from National Science Centre (grant number 2015/19/B/NZ7/02380), D.D. acknowledge support from National Science Center (grant number 2018/30/E/NZ1/00099)

References

1. Crémet, L., Corvec, S., Batard, E., Auger, M., Lopez, I., Pagniez, F., Dauvergne, S., Caroff, N.: Comparison of three methods to study biofilm formation by clinical strains of Escherichia coli. Diagn. Microbiol. Infect. Dis. 75, 252–255 (2013). https://doi.org/10.1016/j.diagmicrobio.2012.11.019.
2. Tenaillon, O., Skurnik, D., Picard, B., Denamur, E.: The population genetics of commensal Escherichia coli, (2010). https://doi.org/10.1038/nrmicro2298.
3. Malanovic, N., Ön, A., Pabst, G., Zellner, A., Lohner, K.: Octenidine: Novel insights into the detailed killing mechanism of Gram-negative bacteria at a cellular and molecular level. Int. J. Antimicrob. Agents. 56, 106146 (2020). https://doi.org/10.1016/j.ijantimicag.2020.106146.
4. Alvarez-Marin, R., Aires-de-Sousa, M., Nordmann, P., Kieffer, N., Poirel, L.: Antimicrobial activity of octenidine against multidrug-resistant Gram-negative pathogens. Eur. J. Clin. Microbiol. Infect. Dis. 36, 2379–2383 (2017). https://doi.org/10.1007/s10096-017-3070-0.
5. Koburger, T., Hubner, N.-O., Braun, M., Siebert, J., Kramer, A.: Standardized comparison of antiseptic efficacy of triclosan, PVP-iodine, octenidine dihydrochloride, polyhexanide and chlorhexidine digluconate. J. Antimicrob. Chemother. 65, 1712–1719 (2010). https://doi.org/10.1093/jac/dkq212.
6. Wang, X., Quinn, P.J.: Endotoxins: Lipopolysaccharides of gram-negative bacteria. Subcell. Biochem. 53, 3–25 (2010). https://doi.org/10.1007/978-90-481-9078-2_1.
7. Raetz, C.R.H., Whitfield, C.: Lipopolysaccharide endotoxins, (2002). https://doi.org/10.1146/annurev.biochem.71.110601.135414.
8. Ebbensgaard, A., Mordhorst, H., Aarestrup, F.M., Hansen, E.B.: The Role of Outer Membrane Proteins and Lipopolysaccharides for the Sensitivity of Escherichia coli to Antimicrobial Peptides. Front. Microbiol. 9, 2153 (2018). https://doi.org/10.3389/fmicb.2018.02153.
9. Erridge, C., Bennett-Guerrero, E., Poxton, I.R.: Structure and function of lipopolysaccharides, (2002). https://doi.org/10.1016/S1286-4579(02)01604-0.
10. Sohlenkamp, C., Geiger, O.: Bacterial membrane lipids: Diversity in structures and pathways, (2015). https://doi.org/10.1093/femsre/fuv008.
11. Epand, R.M., Epand, R.F.: Lipid domains in bacterial membranes and the action of antimicrobial agents, (2009). https://doi.org/10.1016/j.bbamem.2008.08.023.
12. De Vivo, M., Masetti, M., Bottegoni, G., Cavalli, A.: Role of Molecular Dynamics and Related Methods in Drug Discovery, (2016).

ICCS Camera Ready Version 2021
To cite this paper please use the final published version:
DOI: 10.1007/978-3-030-77964-1_42

https://doi.org/10.1021/acs.jmedchem.5b01684.
13. Wu, E.L., Engström, O., Jo, S., Stuhlsatz, D., Yeom, M.S., Klauda, J.B., Widmalm, G., Im, W.: Molecular dynamics and NMR spectroscopy studies of E. coli lipopolysaccharide structure and dynamics. Biophys. J. 105, 1444–1455 (2013). https://doi.org/10.1016/j.bpj.2013.08.002.
14. Hwang, H., Paracini, N., Parks, J.M., Lakey, J.H., Gumbart, J.C.: Distribution of mechanical stress in the Escherichia coli cell envelope. Biochim. Biophys. Acta - Biomembr. 1860, 2566–2575 (2018). https://doi.org/10.1016/j.bbamem.2018.09.020.
15. Piggot, T.J., Holdbrook, D.A., Khalid, S.: Conformational dynamics and membrane interactions of the E. coli outer membrane protein FecA: A molecular dynamics simulation study. Biochim. Biophys. Acta - Biomembr. 1828, 284–293 (2013). https://doi.org/10.1016/j.bbamem.2012.08.021.
16. Chen, J., Zhou, G., Chen, L., Wang, Y., Wang, X., Zeng, S.: Interaction of Graphene and its Oxide with Lipid Membrane: A Molecular Dynamics Simulation Study. J. Phys. Chem. C. 120, 6225–6231 (2016). https://doi.org/10.1021/acs.jpcc.5b10635.
17. Wu, E.L., Cheng, X., Jo, S., Rui, H., Song, K.C., Dávila-Contreras, E.M., Qi, Y., Lee, J., Monje-Galvan, V., Venable, R.M., Klauda, J.B., Im, W.: CHARMM-GUI membrane builder toward realistic biological membrane simulations, (2014). https://doi.org/10.1002/jcc.23702.
18. Kanonenberg, K., Royes, J., Kedrov, A., Poschmann, G., Angius, F., Solgadi, A., Spitz, O., Kleinschrodt, D., Stühler, K., Miroux, B., Schmitt, L.: Shaping the lipid composition of bacterial membranes for membrane protein production. Microb. Cell Fact. 18, 131 (2019). https://doi.org/10.1186/s12934-019-1182-1.
19. Szatmári, D., Sárkány, P., Kocsis, B., Nagy, T., Miseta, A., Barkó, S., Longauer, B., Robinson, R.C., Nyitrai, M.: Intracellular ion concentrations and cation-dependent remodelling of bacterial MreB assemblies. Sci. Rep. 10, 12002 (2020). https://doi.org/10.1038/s41598-020-68960-w.
20. Strauss, J., Burnham, N.A., Camesano, T.A.: Atomic force microscopy study of the role of LPS O-antigen on adhesion of E. coli. J. Mol. Recognit. 22, 347–355 (2009). https://doi.org/10.1002/jmr.955.
21. Wu, E.L., Fleming, P.J., Yeom, M.S., Widmalm, G., Klauda, J.B., Fleming, K.G., Im, W.: E. coli outer membrane and interactions with OmpLA. Biophys. J. 106, 2493–2502 (2014). https://doi.org/10.1016/j.bpj.2014.04.024.
22. Klauda, J.B., Venable, R.M., Freites, J.A., O'Connor, J.W., Tobias, D.J., Mondragon-Ramirez, C., Vorobyov, I., MacKerell, A.D., Pastor, R.W.: Update of the CHARMM All-Atom Additive Force Field for Lipids: Validation on Six Lipid Types. J. Phys. Chem. B. 114, 7830–7843 (2010). https://doi.org/10.1021/jp101759q.
23. Abraham, M.J., Murtola, T., Schulz, R., Páll, S., Smith, J.C., Hess, B., Lindah, E.: Gromacs: High performance molecular simulations through multi-level parallelism from laptops to supercomputers. SoftwareX. 1–2, 19–25 (2015). https://doi.org/10.1016/j.softx.2015.06.001.
24. Guixà-González, R., Rodriguez-Espigares, I., Ramírez-Anguita, J.M., Carrió-Gaspar, P., Martinez-Seara, H., Giorgino, T., Selent, J.: MEMBPLUGIN: studying membrane complexity in VMD. Bioinformatics. 30, 1478–1480 (2014). https://doi.org/10.1093/bioinformatics/btu037.

ICCS Camera Ready Version 2021
To cite this paper please use the final published version:
DOI: 10.1007/978-3-030-77964-1_42

25. Giorgino, T.: Computing diffusion coefficients in macromolecular simulations: the Diffusion Coefficient Tool for VMD. J. Open Source Softw. 4, 1698 (2019). https://doi.org/10.21105/joss.01698.
26. Vanegas, J.M., Torres-Sánchez, A., Arroyo, M.: Importance of force decomposition for local stress calculations in biomembrane molecular simulations. J. Chem. Theory Comput. 10, 691–702 (2014). https://doi.org/10.1021/ct4008926.
27. Bacle, A., Gautier, R., Jackson, C.L., Fuchs, P.F.J., Vanni, S.: Interdigitation between Triglycerides and Lipids Modulates Surface Properties of Lipid Droplets. Biophys. J. 112, 1417–1430 (2017). https://doi.org/10.1016/j.bpj.2017.02.032.
28. Drabik, D., Chodaczek, G., Kraszewski, S., Langner, M.: Mechanical Properties Determination of DMPC, DPPC, DSPC, and HSPC Solid-Ordered Bilayers. Langmuir. 36, 3826–3835 (2020). https://doi.org/10.1021/acs.langmuir.0c00475.
29. Doktorova, M., LeVine, M. V., Khelashvili, G., Weinstein, H.: A New Computational Method for Membrane Compressibility: Bilayer Mechanical Thickness Revisited. Biophys. J. 116, 487–502 (2019). https://doi.org/10.1016/j.bpj.2018.12.016.
30. Marsh, D.: Lateral pressure profile, spontaneous curvature frustration, and the incorporation and conformation of proteins in membranes. Biophys. J. 93, 3884–3899 (2007). https://doi.org/10.1529/biophysj.107.107938.
31. Devanand, T., Krishnaswamy, S., Vemparala, S.: Interdigitation of Lipids Induced by Membrane–Active Proteins. J. Membr. Biol. 252, 331–342 (2019). https://doi.org/10.1007/s00232-019-00072-7.
32. Shearer, J., Khalid, S.: Communication between the leaflets of asymmetric membranes revealed from coarse-grain molecular dynamics simulations. Sci. Rep. 8, 1805 (2018). https://doi.org/10.1038/s41598-018-20227-1.
33. Hsu, P.C., Samsudin, F., Shearer, J., Khalid, S.: It Is Complicated: Curvature, Diffusion, and Lipid Sorting within the Two Membranes of Escherichia coli. J. Phys. Chem. Lett. 8, 5513–5518 (2017). https://doi.org/10.1021/acs.jpclett.7b02432.
34. Domínguez-Medina, C.C., Pérez-Toledo, M., Schager, A.E., Marshall, J.L., Cook, C.N., Bobat, S., Hwang, H., Chun, B.J., Logan, E., Bryant, J.A., Channell, W.M., Morris, F.C., Jossi, S.E., Alshayea, A., Rossiter, A.E., Barrow, P.A., Horsnell, W.G., MacLennan, C.A., Henderson, I.R., Lakey, J.H., Gumbart, J.C., López-Macías, C., Bavro, V.N., Cunningham, A.F.: Outer membrane protein size and LPS O-antigen define protective antibody targeting to the Salmonella surface. Nat. Commun. 11, 1–11 (2020). https://doi.org/10.1038/s41467-020-14655-9.
35. Piggot, T.J., Holdbrook, D.A., Khalid, S.: Electroporation of the E. coli and S. aureus membranes: Molecular dynamics simulations of complex bacterial membranes. J. Phys. Chem. B. 115, 13381–13388 (2011). https://doi.org/10.1021/jp207013v.
36. Camley, B.A., Lerner, M.G., Pastor, R.W., Brown, F.L.H.: Strong influence of periodic boundary conditions on lateral diffusion in lipid bilayer membranes. J. Chem. Phys. 143, 243113 (2015). https://doi.org/10.1063/1.4932980.
37. Jefferies, D., Shearer, J., Khalid, S.: Role of O-Antigen in Response to Mechanical Stress of the E. coli Outer Membrane: Insights from Coarse-Grained MD Simulations. J. Phys. Chem. B. 123, 3567–3575 (2019). https://doi.org/10.1021/acs.jpcb.8b12168.

ICCS Camera Ready Version 2021
To cite this paper please use the final published version:
DOI: 10.1007/978-3-030-77964-1_42